

N O T I C E

THIS DOCUMENT HAS BEEN REPRODUCED FROM
MICROFICHE. ALTHOUGH IT IS RECOGNIZED THAT
CERTAIN PORTIONS ARE ILLEGIBLE, IT IS BEING RELEASED
IN THE INTEREST OF MAKING AVAILABLE AS MUCH
INFORMATION AS POSSIBLE

DOE/NASA/0201/3
NASA CR-165304

EVALUATION OF DISTRIBUTED GAS COOLING OF PRESSURIZED PAFC FOR UTILITY POWER GENERATION

THIRD QUARTERLY REPORT: MARCH 1981 - MAY 1981

M. Farooque, H. Maru, A. Skok
ENERGY RESEARCH CORPORATION
3 Great Pasture Road
Danbury, CT 06810

May 1981

Prepared for
NATIONAL AERONAUTICS AND SPACE ADMINISTRATION
Lewis Research Center
Under Contract DEN3-201



for

U.S. DEPARTMENT OF ENERGY
Energy Technology
Division of Fossil Fuel Utilization
Under Interagency Agreement DEAI-03-80E717088

TABLE OF CONTENTS

		<u>Page No.</u>
	1. EXECUTIVE SUMMARY.....	1
	2. TECHNICAL PROGRESS.....	2
TASK I.	<u>DESIGN AND CONSTRUCTION OF TEST EQUIPMENT FOR 12 x 17 in. (1200 cm²) STACK TESTING.....</u>	2
I.1	CONSTRUCTION OF TEST STATION.....	2
TASK II.	<u>TESTING AND EVALUATION OF 5 x 15 in. (350 cm²) SHORT STACKS...</u>	3
II.1	PRESSURE TESTING OF STACK P5-2.....	3
II.2	TESTING OF STACK P5-3.....	9
TASK III.	<u>PERFORMANCE TESTING OF RECIRCULATED GAS COOLED 12 x 17 in. (1200 cm²) FUEL CELL STACKS.....</u>	16
III.1	DESIGN OF STACKS P12-1 and P12-2....	16
TASK IV.	<u>DESIGN TESTING AND EVALUATION OF DIGAS COOLED 12 x 17 in. 10 kW, FUEL CELL STACKS.....</u>	16
IV.1	COOLING PLATE DESIGN.....	16

LIST OF FIGURES

<u>Figure No.</u>		<u>Page No.</u>
II.1	PRESSURIZED AND ATMOSPHERIC PERFOR- MANCES OF STACK P5-2.....	4
II.2	PRESSURIZED LIFEGRAPH OF STACK P5-2....	8
II.3	TEMPERATURE PROFILE OF STACK P5-2 IN THE AIR FLOW DIRECTION.....	10
II.4	PRESSURE EFFECT ON THE TEMPERATURE PROFILE IN THE STACKING DIRECTION.....	11
II.5	AIR FLOW RATE VS PRESSURE DROP, STACK P5-3.....	14
II.6	EFFECT OF OPERATING PRESSURE ON THE AIR SIDE PRESSURE DROP, STACK P5-3.....	15
IV.1	CHANNEL GEOMETRY FOR TREED DESIGN.....	20
IV.2	TEMPERATURE DISTRIBUTIONS FOR PRES- SURIZED STACKS IN THE OXIDANT FLOW DIRECTION.....	26

LIST OF TABLES

<u>Table No.</u>		<u>Page No.</u>
II.1	COMPARISON OF STARTUP PROCEDURES.....	6
II.2	PEAK PERFORMANCE OF STACK P5-3.....	12
II.3	PRESSURIZED GAIN, STACK P5-3.....	12
II.4	RESISTANCE OF STACK P5-3.....	13
IV.1	COMPARISON OF DIFFERENT COOLING PLATE DESIGNS ON NET VOLTAGE BASIS.....	23
IV.2	RESULTS FOR DESIGN 5ZT.....	24

1. EXECUTIVE SUMMARY

The objective of this program is to provide a proof-of-concept test of a gas-cooled pressurized phosphoric acid fuel cell (PAFC). After initial feasibility tests in shorter stacks, 10-kW stacks will be tested. Progress made in different task areas during the third quarter of the program is summarized below:

Design and Construction of Test Equipment for 12 x 17 in. (1200 cm²) Stack Testing

Excepting a flowmeter, all purchased parts are received and the construction of the test station is 70% completed.

Testing and Evaluation of 5 x 15 in. (350 cm²) Short Stacks

Two short stacks were pressure tested at 446 kPa (4.4 atm.) and the pressure gains were more than the theoretically predicted gains. Temperature profiles were observed to be independent of operating pressure. The pressure drop was found to be inversely proportional to operating pressure as expected. Continuous pressurized operation of a stack for 1000 hours verified the compatibility of the fuel cell component design. A simple pressurization procedure has also been developed.

Design Testing and Evaluation of Gas Cooled 12 x 17 in. (1200 cm²) 10 kW, Fuel Cell Stacks

Six separate designs, covering two gas cooling schemes (DIGAS and separated) and two cooling channel geometries (straight through and treed), were analysed on the net voltage output basis. "Separated" cooling (in "separated" cooling process air and the cooling streams flow separately through the stack.) with 5 cells per cooler was recognized to be the best among the designs considered and will be employed in the first 10 kW fuel cell stack.

2. TECHNICAL PROGRESS

TASK 1. DESIGN AND CONSTRUCTION OF TEST EQUIPMENT FOR 12 x 17 in. (1200 cm²) STACK TESTING

This quarter the flanges and piping for the recirculation loop were received. The piping was cut to the proper size and the flanges were welded in place. The blower was received and installation of the recirculation loop has begun.

The main pressure vessel, heat exchanger, and smaller condenser vessels were received and inspected and are waiting to be connected to the panel.

Most of the components for the Data Acquisition system (DAS) have been received. Software is being written and the system's components are being interfaced and initialized. Wiring to the test facilities is tentatively scheduled for July.

The control panel was received and the control instruments were mounted in the panel. Gas plumbing, electrical wiring, and pneumatic calibration were also completed. The power supply for the blower speed control was received and installed. The safety circuit and load bank were designed and all parts were ordered. The safety circuit and load bank are scheduled for completion by end of June. The construction is progressing according to schedule and the test facility is expected to be ready by early July.

TASK II. TESTING AND EVALUATION OF 350 cm² (5 x 15 in.) SHORT STACKS

II.1 PRESSURE TESTING OF STACK P5-2*

The modification of the available test station, required for pressure testing 6-cell 350 cm² stacks, was completed. After 960 hours of atmospheric testing, Stack P5-2, was successfully pressurized to 446 kPa in this station. Pressurization was performed at a slow rate (≈ 2 kPa/min), low load (50 mA/cm²) and in two stages. All six cells achieved significant gain in performance.

Average performances of this stack at atmospheric and at pressurized conditions are compared in Figure II.1. Theoretical gain due to pressurization (Nernst and cathode polarization) is:

$$\begin{aligned}\Delta V &= 1.5 \frac{RT}{F} \ln \frac{P_2}{P_1} \\ &= 0.089 \text{ V for } P_2 = 446 \text{ kPa (4.4 atm.)}\end{aligned}$$

From the experimental results (Figure II.1) it is visible that the observed gain in terminal voltage is higher than the theoretically predicted gain and in addition to this, the performance gain is current density dependent. These observations can be explained from the facts that:

1. At atmospheric conditions and at current densities higher than 150 mA/cm² some diffusion loss is present. Pressurized operation leads to reduction in the diffusion loss via increasing the oxygen reduction limiting current density, because oxygen partial pressure increases due to pressurization.

* Progress Report No. 6, Dec.-Feb. 1980.

- Atmospheric (after 960 hours of testing)
- △ 446 kPa (Initial pressurization)
- 446 kPa (after 1000 hours of pressurization)

Stack P5-2
 (6 cells w/ straight thru cooling plate
 & 3 cells have AlCM)
 Stack Resistance: 4.8 mΩ
 Air Utilization: 50% (calc.)
 Hydrogen Utilization: 80%

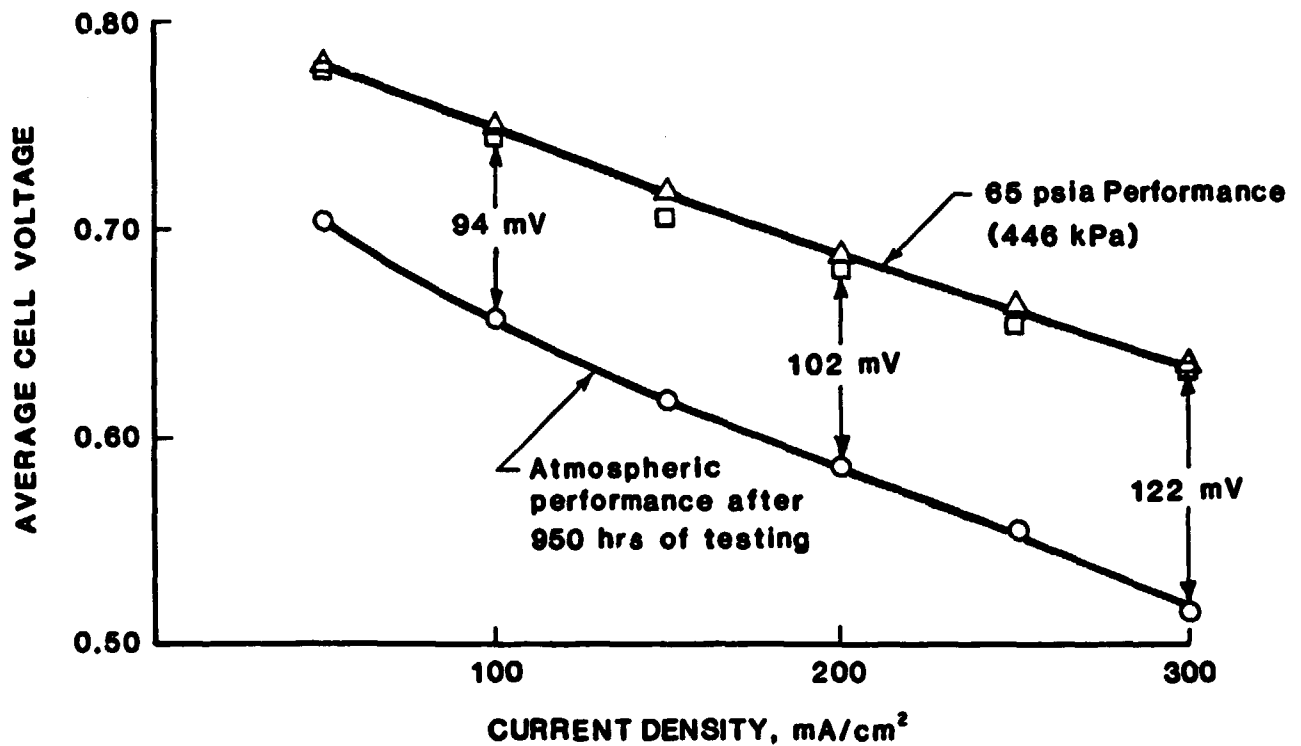


FIGURE II.1: PRESSURIZED AND ATMOSPHERIC PERFORMANCES OF STACK P5-2

2. As a result of pressurization to 445 kPa (65 psia) the average acid concentration drops from 100.8 wt% to 96.6 wt%. Since 96.6% acid has higher ionic conductivity, the stack resistance goes down. Out of the observed 1.0 m Ω drop in cell resistance resulting from pressurization, about 0.2 m Ω can be attributed to the increased acid conductivity (calculated from Macdonald & Boyack's data*). The remaining 0.8 m Ω is probably related to better wetting of the cell matrix as a result of acid volume expansion caused by pressurization, calculated to be about 7.8%. At an operating current density of 300 mA/cm² 1.0 m Ω drop in cell voltage will produce a performance gain of 96V for the stack (16 mV per cell). Note that the Stack P5-2 was tested for 960 hours at atmospheric conditions prior to pressurization without acid addition (the stack started indicating symptoms of acid starvation), and the pressurization was performed without adding any acid.

In the initial pressurization run, a previously developed conservative pressurization scheme was successfully implemented. After 240 hours of pressure testing, the stack was depressurized for acid addition (1 cm³ per cell). Next the stack was repressurized successfully using a newly developed, faster and more practicable pressurization scheme. The main features of these methods are compared in Table II.1. In the newly developed method pressurization is accomplished under no-load conditions, therefore the differential pressure over-shooting during transients are minimized (because very small net flow is involved). Furthermore, under no-load conditions the blower in the recirculating loop need not be run at pressures lower than the design pressure; therefore, blower design becomes much simpler.

* David I. Macdonald and James P. Boyack, Journal of Chemical Engineering Data, Vol. 14, No. 3, July 1969.

TABLE II.1 COMPARISON OF STARTUP PROCEDURES

Features	Previously Developed Method	Newly Developed Method
Pressurization Rate*	2 kPa/min	4 kPa/min
Current Density	$\approx 50 \text{ mA/cm}^2$	No Load
Steps	Multistep	One Step
Cell Temperature	Normal Cell Temp.	Low Cell Temp. $\approx 150^\circ\text{C}$
Advantages & Disadvantages	Inherently slow because of acid dilution and transient differential pressure considerations. Requires continuous operation of the coolant recirculation blower.	Corrosion rate is comparable. Pressurization is faster. Blower design will be simpler. Differential pressure control during transient becomes simpler.

* Represent the experimentally used rate. Optimum rate will probably be faster.

Although the stack is submitted to the open circuit condition, the corrosion rate is comparable to the normal running conditions, because low stack temperature is maintained during pressurization. In future experiments, attempts will be made to optimize the pressurization rate and also to develop a practicable shutdown procedure.

Stack P5-2 had undergone one normal depressurization - pressurization cycle after about 240 hours of pressure testing and an emergency shutdown cycle after 330 hours of operation. The testing of Stack P5-2 was terminated for post-test analyses after it has completed a total of 1000 hours of pressure testing. Note that the total testing life of this stack is 2300 hours. Polarization plot taken at two different times are compared in Figure II.1. Only a slight decay in performance ($3 \text{ mV @ } 100 \text{ mA/cm}^2$) is observed. The stack performance at all current densities are stable. Therefore, the long term (1000 hours) pressurization effect on performance appears to be negligible. The total stack resistance has gone up from $5.4 \text{ m}\Omega$ to $35 \text{ m}\Omega$ and the post-test analyses revealed a loose connection in the positive terminal of the cell. The pressurization lifograph of the stack as shown in Figure II.2 indicates a stable pressurized performance. The cooler resistance stayed unchanged at $0.18 \text{ m}\Omega$ (note that cooler resistance was also the same when atmospheric testing was started).

Post-test analyses of Stack P5-3 did not expose incompatibility of any one of the state-of-the-art atmospheric fuel cell components for pressurized operations. Bipolar plates and cooler plates remained dry, normal and reusable. Backing papers were observed to be slightly over compressed, at one corner, without any apparent adverse effect on the cell performance.

The temperature distribution in both the air flow and the stacking direction was measured using an array of 14 thermocouples. Temperature profiles obtained in the air flow direction

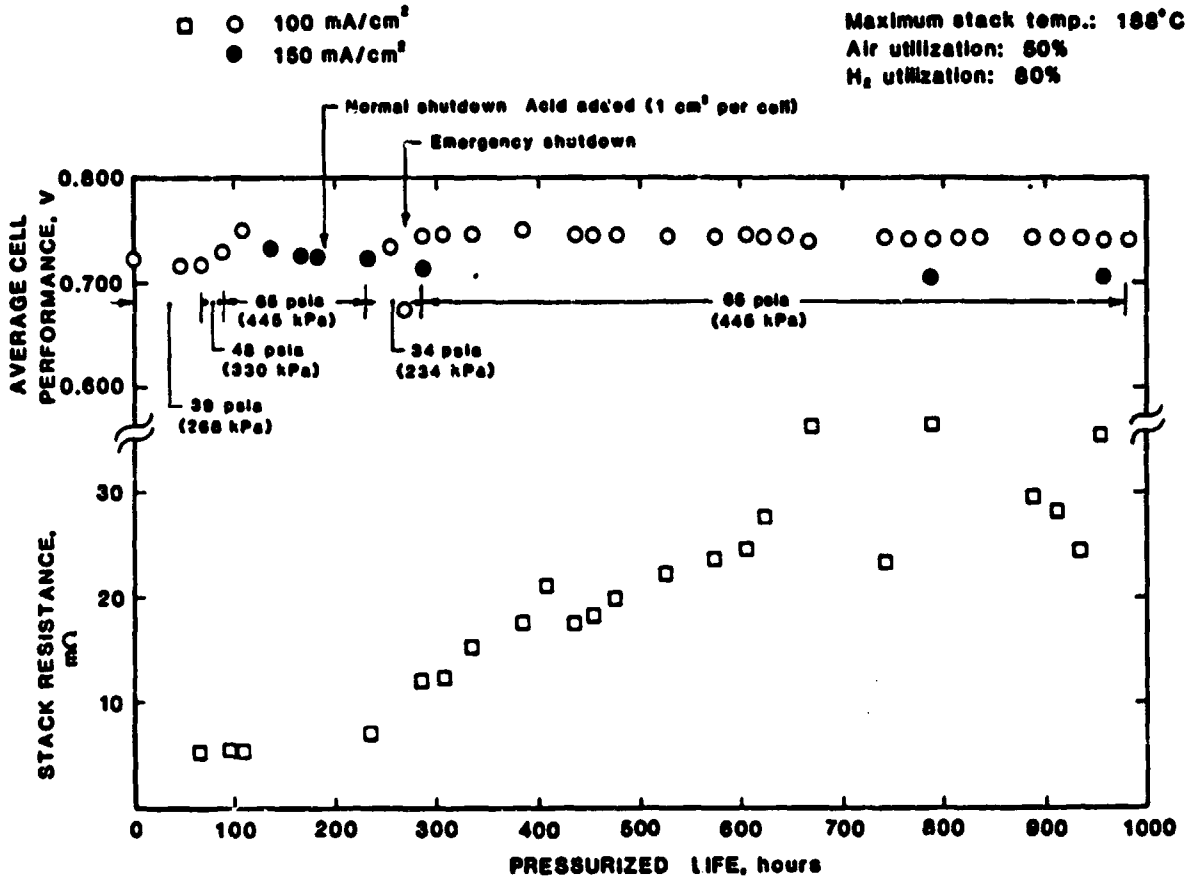


FIGURE II.2 LIFEGRAPH OF PRESSURIZED STACK P5-2
(PRIOR TO PRESSURIZATION, THE STACK WAS TESTED UNDER
ATMOSPHERIC CONDITIONS FOR 960 HRS.)

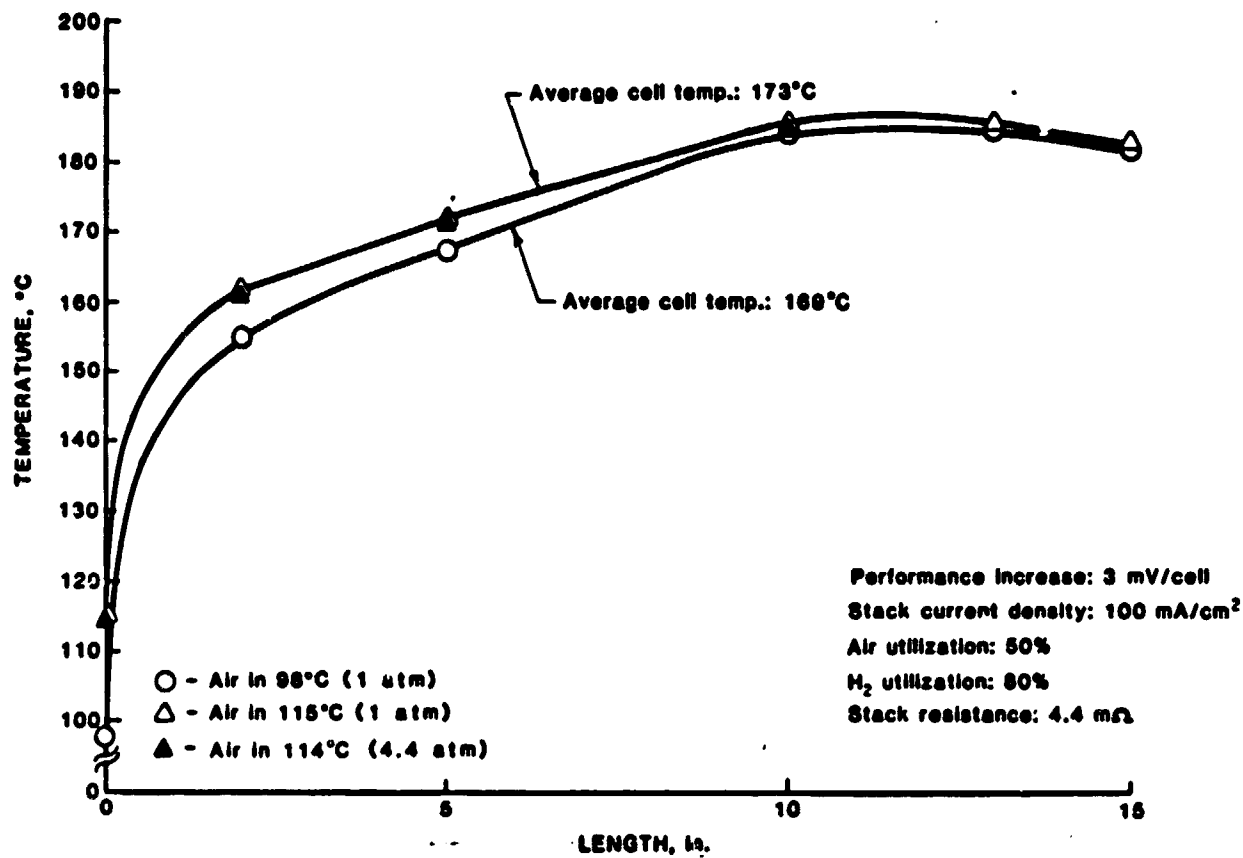
D1613

at two different air inlet conditions are shown in Figure II.3. As is expected for straight through cooling channels, a large temperature gradient exists and the inlet section of the stack is significantly colder. Increasing the inlet air temperature by 17°C (from 98°C to 115°C) improved the average cell temperature (calculated by the Trapezoidal Rule) by 4°C (from 169°C to 173°C) and the improvement in stack performance was only 18 mV. Figure II.3 also shows that the temperature in the air flow direction is independent of fuel cell operating pressure. Temperature profiles obtained in the stacking direction, at two different pressures (all other experimental conditions are the same), are compared in Figure II.4. These results indicate a very small temperature gradient ($T_{\text{max}} - T_{\text{min}} \leq 3^{\circ}\text{C}$) in the stacking direction which is also independent of the operating pressure.

II.2 TESTING OF STACK P5-3

The assembly of Stack P5-3 (identical to P5-2 in design) was completed. The stack was initially tested at atmospheric conditions for 500 hours and the peak performance is summarized in Table II.2. All the cells, including the ones with AICMs, have reasonable performance. As was observed in the previous stack (P5-2), the cells with AICMs have low OCVs. After 500 hours of atmospheric testing the stack was pressurized to 446 kPa (65 psia). The observed pressurized gains are summarized in Table II.3.

Previously stack resistance was observed to change with aging, pressurization, etc. To understand this, a new experimental procedure has been instituted which allows the monitoring of individual cell and current collector resistances. The results as summarized in Table II.4 indicate lower resistance for the cells assembled with AICM. The average reduction in cell resistance caused by pressurization to 446 kPa is 0.12 mΩ.



D15468

FIGURE II.3 TEMPERATURE PROFILE OF STACK P5-2
IN THE AIR FLOW DIRECTION

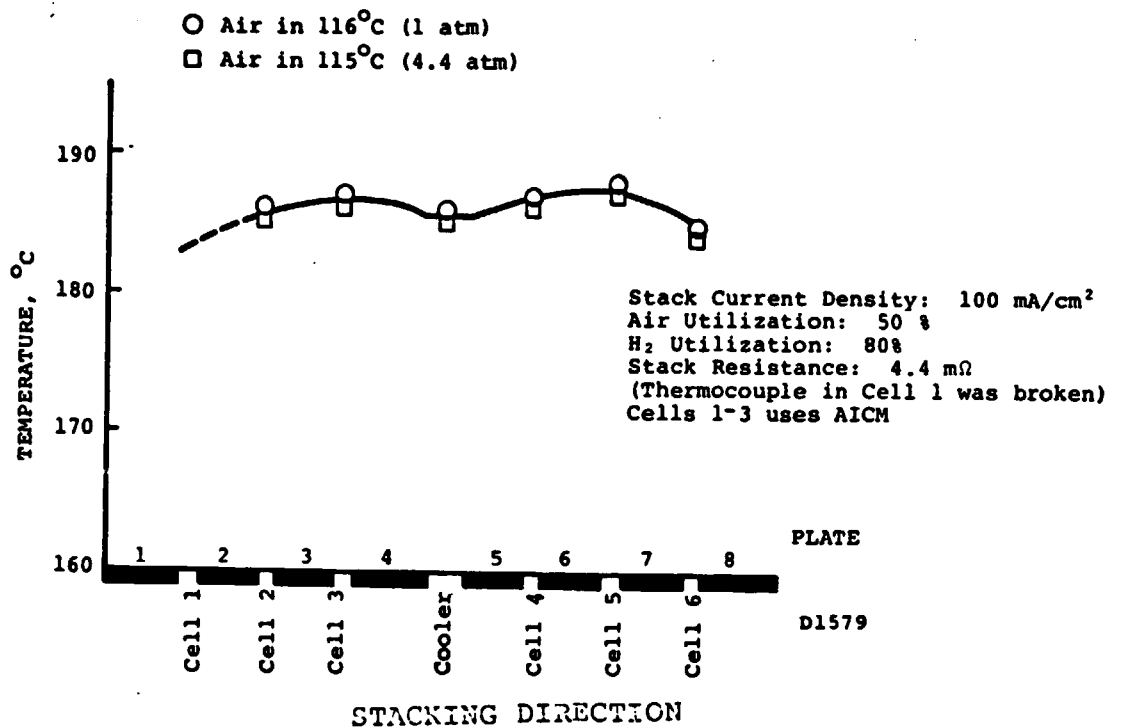


FIGURE II.4 PRESSURE EFFECT ON THE TEMPERATURE PROFILE IN THE STACKING DIRECTION

ENERGY RESEARCH CORPORATION

TABLE II.2 PEAK PERFORMANCE OF STACK P5-3

Cell No.	Performance*, after 150 hours, V	
	@ 150 mA/cm ²	OCV
1	0.66	0.81
2	0.65	0.80
3	0.66	0.81
4	0.64	0.86
5	0.64	0.84
6	0.63	0.87
TOTAL	3.87	4.99
AVG. Per Cell	0.645	0.83

*Stack resistance** : 4.2 + 1.2 = 5.4 mΩ

Air Temperature : 113°C (in), 179°C (out)

H₂ Temperature : 118°C (in), 156°C (out)

Stack Temperature : 124°C

Air Flow Rate : 40 lpm (2 S through process channel)

H₂ Flow Rate : 1.87 lpm (80% H₂ utilization)

**Resistance contributed by the current collectors and the terminals is 1.2 mΩ.

TABLE II.3 PRESSURIZED GAIN, STACK P5-3

CURRENT DENSITY mA/cm ²	PRESSURIZED GAIN @ 445 kPa (65 psia) (per cell), mV
100	94
150	97
200	108
250	112
300	133

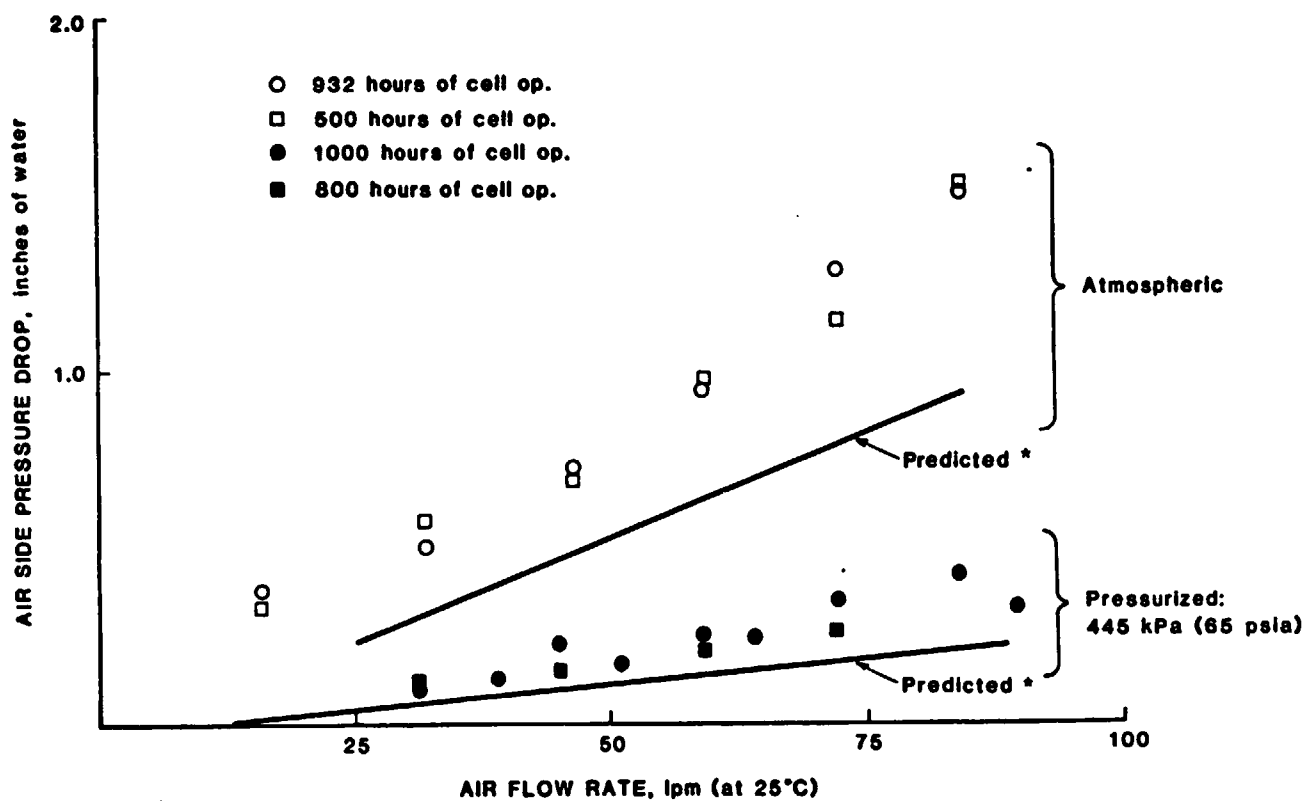
TABLE II.4 RESISTANCE OF STACK P5-3

OPERATING PRESSURE kPa	RESISTANCE, m Ω									TOTAL (MEASURED)
	POSITIVE TERMINAL	AICM			COOLER	STANDARD			NEGATIVE TERMINAL	
		CELL 1	CELL 2	CELL 3		CELL 4	CELL 5	CELL 6		
101 (1 atm)	0.69	0.42	0.38	0.42	0.30	0.62	0.59	0.71	0.68	5.0
446 (4.4 atm)	0.70	0.33	0.30	0.34	0.30	0.47	0.44	0.54	0.67	4.2

Pressure drop in the air flow side was continuously monitored for Stack P5-3 and the results are summarized in Figure II.5. Experimentally observed pressure drop is larger than the values predicted by the equations developed at Westinghouse*. Partial blockage of the process channels by the backing paper, due to sagging, may cause reduction in available flow area which may be responsible for the higher observed pressure drops. Experimental pressure drop values (Figure II.6) also confirms that the pressure drop is inversely proportional to the fuel cell operating pressure.

Pressure testing of Stack P5-3 will continue to document the effect of CO and CO₂ on the pressurized performance, and also to study the long-term effects of pressurization on performance and component compatibility.

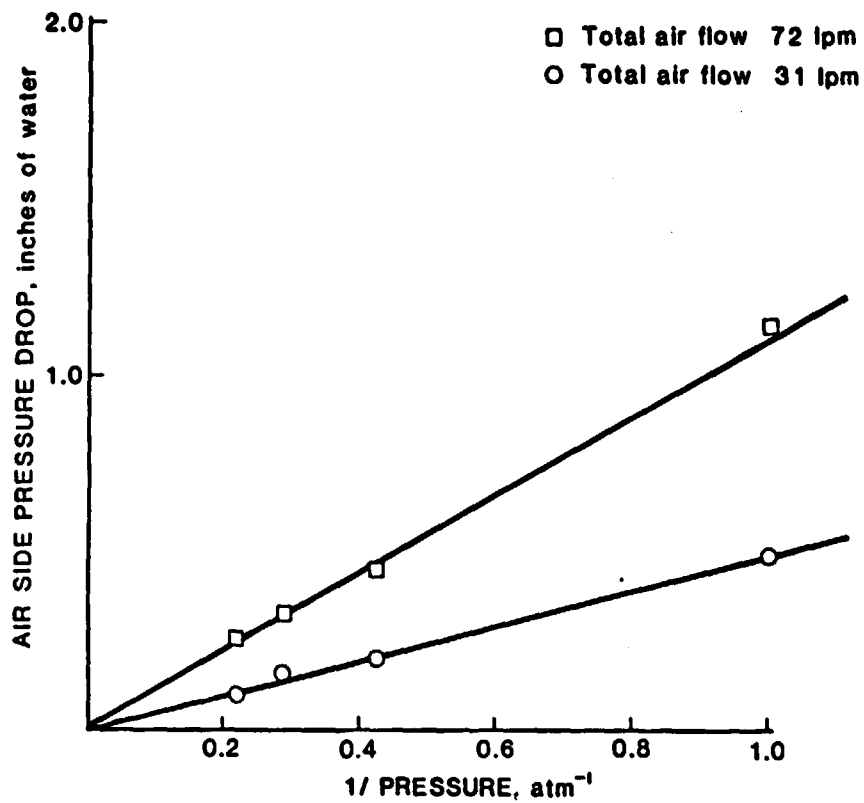
* Westinghouse R&D Center Final Report, Contract Number DE-AC03-78ET11300, February 1980.



D1614

FIGURE II.5 AIR FLOW RATE Vs PRESSURE DROP, STACK P5-3
(@ 65 psia, 2 S through the process channel)

* Were calculated using equations developed in Westinghouse R&D Center Final Report, Contract Number DE-AC03-78ET11300, February 1980.



D1615

FIGURE II.6 EFFECT OF OPERATING PRESSURE ON THE AIR SIDE PRESSURE DROP, STACK P5-3

**TASK III. PERFORMANCE TESTING OF RECIRCULATED GAS
COOLED 12" x 17" (1200 cm²) FUEL CELL STACKS**

III.1 DESIGN OF STACKS P12-1 and P12-2

Design of first two 6-cell 1200 cm² stacks, P12-1 and P12-2, are completed. Both the stacks will have a treed cooler placed at the middle and the separated cooling scheme will be implemented. The cooling plate design is discussed under Task IV. The bipolar plates and the cooling plates are being molded now. After that the plates will be machined. The stacks are expected to be assembled in July.

**TASK IV. DESIGN TESTING AND EVALUATION OF GAS COOLED
12" x 17" 10 kW, FUEL CELL STACKS**

IV.1 COOLING PLATE DESIGN

The objective is to determine the best cooling channel geometry for air cooled, pressurized phosphoric acid fuel cells. The analysis relies heavily on the analytic models and test results developed in the OS/IES program, (NASA contract DEN3-161). Two types of operation of a gas cooled fuel cell stack are considered. These are DIGAS cooling and separated cooling. In the DIGAS design, the makeup air is mixed with the recirculated portion of the stack exit flow before entering the stack. A fraction, λ , of the inlet stream flows through the process channels and provides oxygen for the reaction. The remaining fraction, $1-\lambda$, flows through cooling channels located within cooling plates. Cooling plates also serve as bipolar plates and are located at 3 to 6 cell intervals.

In the separated cooling design there are separate fuel, process air and cooling streams flowing through the stack. Again cooling plates are located at 3 to 6 cell intervals and

also serve as bipolar plates. The separated cooling design permits once through flow of process air which provides higher oxygen concentration and produces higher cell voltage than the DIGAS design when matrix and electrodes with the same properties are used.

Two types of cooling channel designs are considered, straight through and treed. The straight through design has a uniform rectangular cross section along the cooling path. The treed design uses rectangular cross section channels that progressively branch into additional channels of the same depth but of smaller width at selected intervals along the cooling flow direction. This design allows the increase of the intensity of local cooling along the flow path to compensate for the increase of coolant temperature along the path. The lateral spacing of cooling channels within a cooling plate, channel pitch, also varies as a function of position to compensate for non-uniformity of current density due to local differences in reactant composition and temperature.

Six separate cooling designs (described in Table IV.1) were examined using previously developed analytical model. These designs are designated by a number and letter combination. The number 4 or 5 indicates 4 or 5 cells per cooling plate. The letters DT indicate DIGAS with treed cooling, DS indicates DIGAS with straight cooling channels, and ZT indicates Zee or separated cooling with treed channels. A number of system variables were specified as fixed conditions common to all detailed design calculations. These conditions are:

ENERGY RESEARCH CORPORATION

Makeup Air Flow	$X = 2 \text{ stoich}$
H ₂ Utilization	$\eta_F = .70$
Current Density	$i = 300 \text{ mA/cm}^2$
Average Cell Temperature	$\bar{T} = 177 \text{ C}$
Bulk Air Rise	$\Delta_A = 55 \text{ C}$
Pressure	$P_{ATM} = 344 \text{ kPa, (50 psia)}$
Number of Cells per Cooling Plate	$NCPCP = 4,5$
Fuel Composition	$Y_{H_2} = .615$ $Y_{CO} = .005$ $Y_{H_2O} = .180$ $Y_{CO_2} = .200$
Digas Oxidant Inlet Composition	$Y_{O_2} = .10$ $Y_{H_2O} = .18$ $Y_{N_2} = .72$
Zee Oxidant Inlet Composition	$Y_{O_2} = .206$ $Y_{H_2O} = .020$ $Y_{N_2} = .774$
Anode Catalyst Loading	$CLA = .3 \text{ mg/cm}^2$
Cathode Catalyst Loading	$CLC = .5 \text{ mg/cm}^2$
Catalyst Specific Area	$SA = 5 \times 10^5 \text{ cm}^2/\text{g}$

In all these analyses the specific resistance was assumed equal in all cases with a value of $0.4\text{-}\Omega\text{-cm}^2$ at 177°C and varied as:

$$\frac{r}{r_o} = \exp \left(\frac{1500}{T_K} - \frac{1500}{450} \right)$$

where T_K = Temperature, $^\circ\text{K}$

r_o = resistance at 177°C

The catalyst utilization was

$$C_u = 0.26 + 0.0033 (T_K - 450)$$

which agrees closely with C_u values for Stacks 561 and 562*.

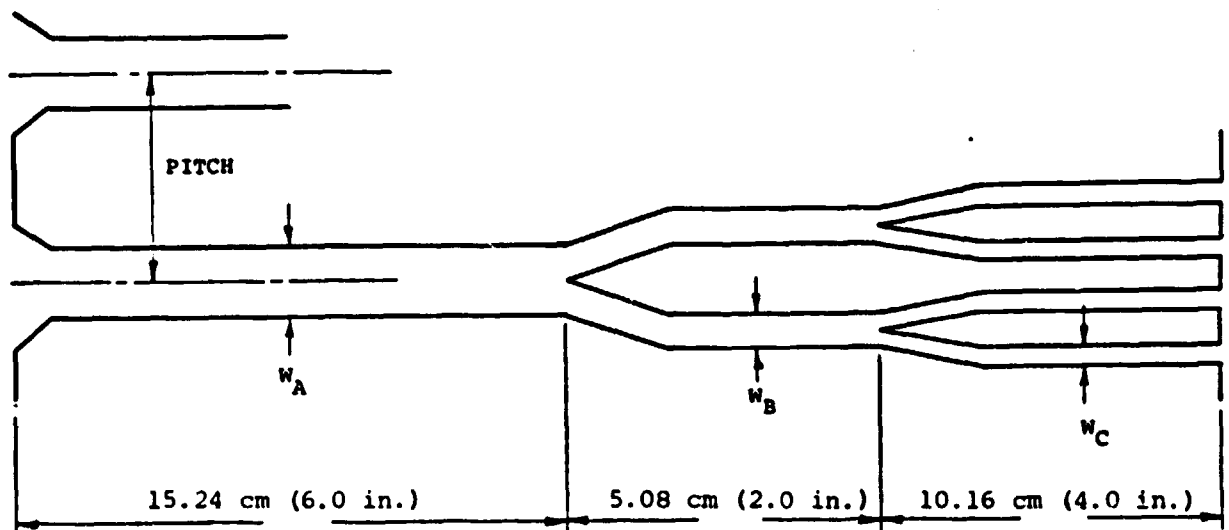
Cooling channels for cases 4DS and 5DS have dimensions specified by current mold geometry. The channels have a uniform pitch of .914 cm (.36 in.) a depth of .254 cm (.10 in.) and mean width of .597 cm (.235 in.). For case 5DS all 44 channels are used. For case 4DS, channel numbers 17, 27, 34 and 41 of the 44 channels are plugged to simulate the desired cooling distribution specified by the calculated results.** The details of treed cooling channel geometry for each case are given in Figure IV.1.

Note that the dimensions of the treed channels were established using the heat transfer considerations (lower heat transfer coefficient at the inlet and higher heat transfer coefficient at the exit, lowest peak to average temperature difference, etc.) and practicable channel dimensions.

The identified optimization criteria for the cooling geometry are pressure drop, cell terminal voltage, and the temperature difference between the average cell temperature

* Technical Progress Report No. 18, Contract DEN3-161, March 1981.

** Channel counting starts from the fuel inlet side.



DESIGN	4 DT. 4ZT	5DT	5ZT	D1575 R
w_a	.508 cm (.200 in.)	.569 cm (.224 in.)	.635 cm (.250 in.)	
w_b	.254 cm (.100 in.)	.284 cm (.112 in.)	.318 cm (.125 in.)	
w_c	.127 cm (.050 in.)	.142 cm (.056 in.)	.159 cm (.063 in.)	
b	.508 cm (.200 in.)	.559 cm (.220 in.)	.559 cm (.220 in.)	
Mean Pitch	1.257 cm (.495 in.)	1.323 cm (.521 in.)	1.270 cm (.500 in.)	

FIGURE IV.1 CHANNEL GEOMETRY FOR TREED DESIGNS

(All dimensions are before heat treatment)

and maximum cell temperature. The terminal voltage of a fuel cell is increased at fixed current density by an increase in average cell temperature. On the other hand, the useful life of cell components is reduced as temperature is increased above limits which depend on the specific materials. Thus for any specified component materials, it is desired to increase the average cell temperature as near as possible to the maximum temperature within the cell.

A logical basis for comparison of all cooling geometries is for each design to have the same peak temperature. Also, since the various designs require differing amounts of parasitic power, the output should be compared on a net power basis. Since at a given current, the output power is directly proportional to cell voltage, it is possible to use net voltage as a measure of net power. If W_c is the parasitic power loss in watts/cell, then the effective voltage loss is

$$\Delta V_c = \frac{W_c}{I}$$

where I is the cell current.

The parasitic losses considered here include only the process air and cooling flows and their respective pressure drops through the stack itself. Other losses are assumed equal and independent of the cooling design.

If each design operates with a specified maximum temperature, T_M , then the average temperature is

$$\bar{T} = T_M - \Delta$$

where Δ is the maximum to average temperature difference or the peak to average gradient. Data for atmospheric pressure

stacks indicate that output voltage changes of about 1.35 mV for each degree C change in stack temperature can be expected at 300 mA/cm². Thus the voltage correction due to the temperature gradient is

$$\Delta V_T = 1.35 (T_M - \Delta - 177)$$

where ΔV_T is in mV and T_M and Δ are in degrees C. A maximum cell temperature of 190°C was assumed.

Table IV.1 shows the calculated voltage, the corrected mean temperatures, the corrections ΔV_T , and the net voltage for each of the six designs. About 22 mV of this difference is due to the use of once through process air and the rest is due to improved temperature uniformity. The straight through DIGAS designs are 20 to 30 mV below the treed DIGAS designs due exclusively to the higher temperature gradient. Design 5ZT i.e., the Zee design with 5 cells per cooling plate therefore appears to be optimum and will be tested in future pressurized stacks. The predicted maximum temperature gradient, peak to average gradient, pressure drops and cell voltages at three different current densities for this design are summarized in Table IV.2.

Although this analysis establishes that the separated cooling is better than the DIGAS scheme, some technology issues such as moldability of the plate design, pressure drop, acid management, etc. need to be resolved. These issues will be addressed under a separate program (DEN3-205).

TABLE IV.1 COMPARISON OF DIFFERENT COOLING PLATE
DESIGNS ON NET VOLTAGE BASIS

(Cell Voltage Corrections for Operation at
Fixed Peak Temperature of 190°C and for
Power Due to Stack Pressure Drops at
Current Density of 300 mA/cm²)

Design	4DS	5DS	4DT	5DT	4ZT	5ZT
Calculated Performance at 177°C (mV)	551	552	552	552	574	574
Corrected Mean Temperature for operation at 190°C (°C)	163	156	180	178	185	185
ΔV_T , (mV)	-18.9	-28.4	+4.1	+1.4	+10.8	+10.8
ΔV_C , (mV)	- 3.6	- 4.3	-3.3	- 1.3	- 2.8	- 2.3
Net Voltage (mV)	529	519	553	550	582	583

TABLE IV.2

RESULTS FOR DESIGN 52T (5 Cells per Cooling
Plate, Zee with Treed Cooling Channels)

Current Density, (mA/cm ²)	200	300	400
Volts per Cell at 177°C (V)	.627	.574	.523
Maximum Gradient T _{max} - T _{min} , (°C)	14.5	20.4	30.9
Peak to Average Gradient, (°C)	7.8	5.1	11.0
Process Air Stoichs	2.0	2.0	2.0
Pressure Drop (cm · H ₂ O)	1.29	2.70	4.64

The temperature distribution along this centerline of the stack for cases 5DS, 5DT and 5ZT are compared in Figure IV.2 at 300 mA/cm² with average temperature of 177°C (350°F) for each case. The corresponding cases for 4 cells per cooler have similar temperature distributions except for a few °C difference in peak to average gradient. Analyses showed that cell voltage at a given current density is essentially independent of the temperature distribution at a common specified average temperature.

Although not discussed here, several cases were also run at other pressures (from 1 to 10 atmospheres). Although voltage increases with pressure and pressure drop decreases with increased pressure, the temperature distributions are virtually independent of pressure. This occurs since viscosity and thermal conductivity are independent of pressure. Thus heat transfer coefficients are also independent of pressure.

3. PROBLEMS

None

4. PLANS

TASK I.

- Completion of test station assembly

TASK II.

- Completion of pressure testing of Stack P5-3
- Pressure testing of Stack P5-4 and P5-5
- Establishment of practicable shutdown procedure, CO₂ and CO effect on pressurized performance, long term effect of pressurization on performance, etc.

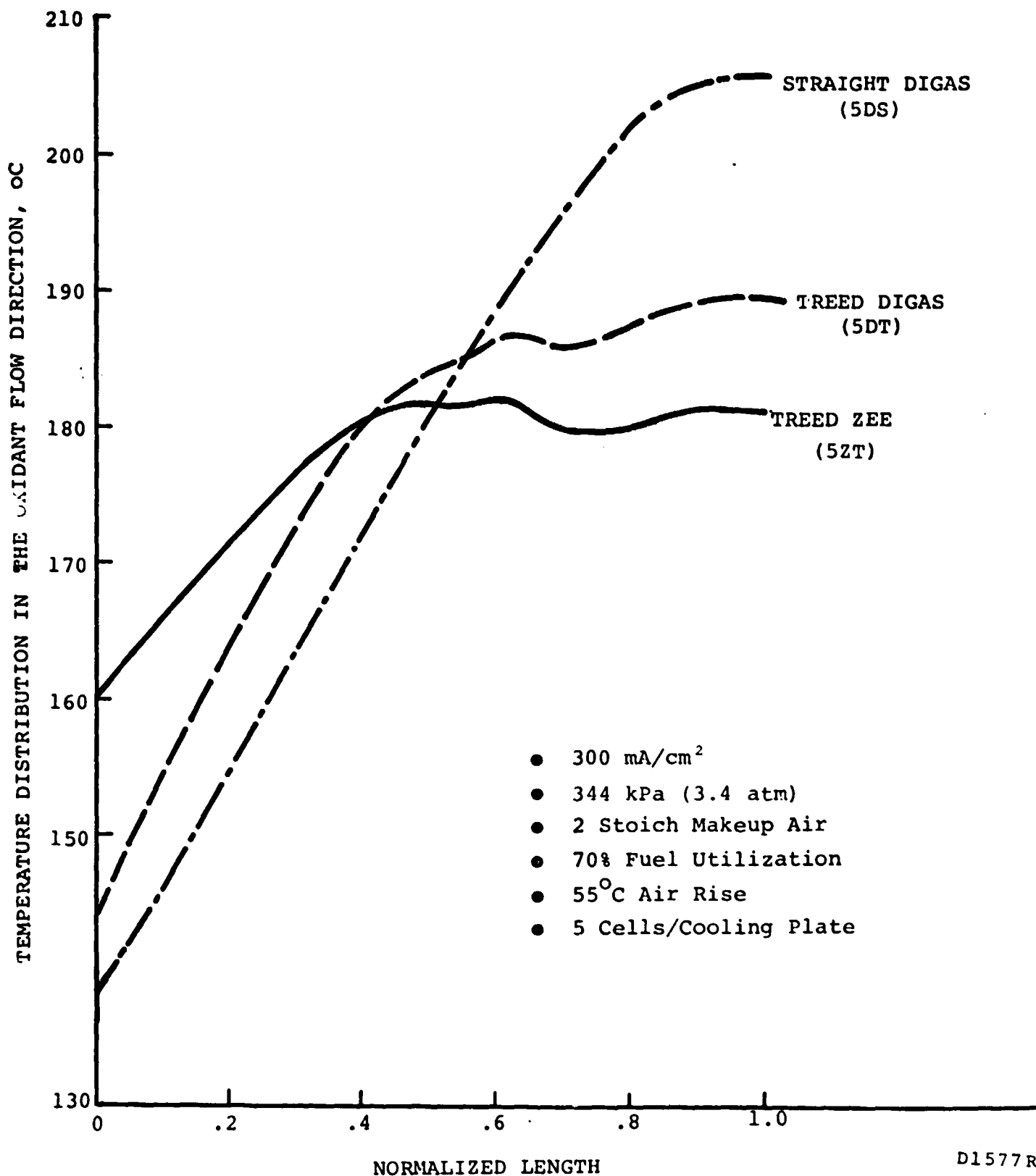


FIGURE IV.2 TEMPERATURE DISTRIBUTIONS FOR PRESSURIZED STACKS IN THE OXIDANT FLOW DIRECTION

(Average Stack Temperature for each case is 177°C)

ENERGY RESEARCH CORPORATION

TASK III.

- Pressure testing of Stack P12-1
- Establishment of baseline pressurized performance at 1010 kPa and temperature profiles.

TASK IV.

- Completion of machining and heat-treatment of bipolar and cooling plates of Stack P10-1